Journal of Advanced Research 28 (2021) 51–62

Contents lists available at ScienceDirect

Journal of Advanced Research

journal homepage: www.elsevier.com/locate/jare

New biodegradable nanoparticles-in-nanofibers based membranes for guided periodontal tissue and bone regeneration with enhanced antibacterial activity

Dina Abdelaziz [a,b], Amr Hefnawy [a], Essam Al-Wakeel [b], Abeer El-Fallal [b,c], Ibrahim M. El-Sherbiny [a,*]

[a] Center for Materials Science (CMS), Zewail City of Science and Technology, 6th of October, Giza 12578, Egypt
[b] Department of Dental Biomaterials, Faculty of Dentistry, Mansoura University, Egypt
[c] Department of Dental Biomaterials, Faculty of Oral and Dental Medicine, Delta University for Science and Technology, Egypt

GRAPHICAL ABSTRACT

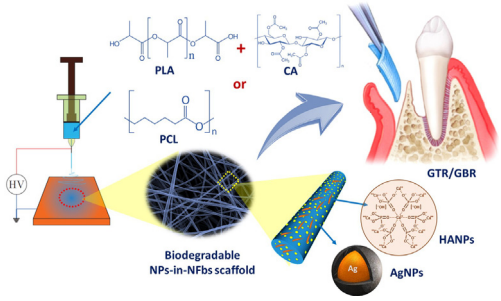

ARTICLE INFO

Article history:
Received 12 March 2020
Revised 12 May 2020
Accepted 17 June 2020
Available online 20 June 2020

Keywords:
Nanoparticles
Nanofibers
GTR
GBR
Periodontal

ABSTRACT

Introduction: Guided tissue regeneration (GTR) and guided bone regeneration (GBR) are commonly used surgical procedures for the repair of damaged periodontal tissues. These procedures include the use of a membrane as barrier to prevent soft tissue ingrowth and to create space for slowly regenerating periodontium and bone. Recent approaches involve the use of membranes/scaffolds based on resorbable materials. These materials provide the advantage of dissolving by time without the need of surgical intervention to remove the scaffolds.
Objectives: This study aimed at preparing a new series of nanofibrous scaffolds for GTR/GBR applications with enhanced mechanical properties, cell adhesion, biocompatibility and antibacterial properties.
Methods: Electrospun nanofibrous scaffolds based on polylactic acid/cellulose acetate (PLA/CA) or poly(caprolactone) (PCL) polymers were prepared and characterized. Different concentrations of green-synthesized silver nanoparticles, AgNPs (1-2% w/v) and hydroxyapatite nanoparticles, HANPs (10-20% w/v) were incorporated into the scaffolds to enhance the antibacterial and bone regeneration activity.
Results: In-vitro studies showed that addition of HANPs improved the cell viability by around 50% for both types of nanofibrous scaffolds. The tensile properties were also improved through addition of 10% HANPs but deteriorated upon increasing the concentration to 20%. AgNPs significantly improved the

Peer review under responsibility of Cairo University.
* Corresponding author at: Zewail City of Science and Technology, Egypt.
E-mail address: ielsherbiny@zewailcity.edu.eg (I.M. El-Sherbiny).

https://doi.org/10.1016/j.jare.2020.06.014
2090-1232/

antibacterial activity with 40 mm inhibition zone after 32 days. Additionally, the nanofibrous scaffolds showed a desirable degradation profile with losing around 40-70% of its mass in 8 weeks.
Conclusions: The obtained results show that the developed nanofibrous membranes are promising scaffolds for both GTR and GBR applications.

Introduction

Periodontitis refers to severe inflammation that may result in the destruction of the periodontium and ultimately tooth loss [1]. There are two main surgical approaches for the regeneration and repair of damaged periodontal tissues which are guided tissue regeneration (GTR) and guided bone regeneration (GBR). In both cases, an occlusive material is used to prevent the growth of connective and epithelial tissues into the defect allowing the regeneration of periodontal tissues [2,3]. Progenitor cells that are located in the neighboring periodontal ligaments, alveolar bone or blood can then migrate to the root area and differentiate into a new periodontal supporting apparatus. These cells form new bone, periodontal ligament (PDL) and cementum. GBR is used to restore deficient alveolar sites (e.g. an extraction site and deficient alveolar ridge) for placement of posterior implant [4].

GTR and GBR involve the use of membranes to support tissue regeneration which requires certain properties for the membranes to allow proper healing. The membranes need to be biocompatible to integrate in the tissues without eliciting inflammatory responses. They must also have a degradation profile that matches the regeneration of the tissues which normally takes around 4–6 weeks. Moreover, their mechanical and physical properties must be suitable for their placement *in-vivo* and their function as a barrier to epithelial and connective tissues growth. They should have high resistance to tear and rupture during surgery [5]. Besides, the membranes should be porous, and the porosity is needed to allow cellular adaptation and sufficient nutrient permeation [6]. Moreover, the membrane should be osteocoductive along with the bone graft. Osteoconductivity refers to the compatibility of the used membrane or scaffold with osteoclasts allowing their growth to form new bone structures starting from the margins of existing bones. Antimicrobial activity is also desirable to prevent infection of the damaged tissues [7].

The need for the aforementioned properties of the membranes for GTR/GBR applications limits the choices regarding the materials. Previously, non-resorbable membranes were used which required surgical intervention to remove the membrane after healing. Resorbable membranes represent more convenient alternatives to the conventional non-resorbable membranes since they degrade by time and do not require surgical removal. They can be made of synthetic polymers such as polylactic acid (PLA), poly (glycolic acid) (PGA), poly(caprolactone) (PCL) or their copolymers. These polymers have excellent biocompatibility, controllable biodegradability, low rigidity, processability, and drug-encapsulating ability. Resorbable membranes may also be fabricated from natural polymers including proteins (e.g., collagen, silk, fibrinogen and elastin), and polysaccharides (e.g., cellulose, chitin and glycosaminoglycans) [8]. Natural polymers are generally considered safer, more biocompatible and more biodegradable compared to synthetic polymers. They also have the ability to present receptor-binding ligands to cells in addition to susceptibility to cell-triggered proteolytic degradation and natural remodeling [9]. However, natural polymers usually suffer from poor mechanical properties that limit their use for such application. For GBR/GTR application, the use of pure synthetic or natural polymer scaffolds is usually unsatisfactory. Pure polymers may have low stiffness, hydrophobic nature or relatively low bioactivity. On the other hand, the degradation products of synthetic polymers are sometimes detrimental for newly grown tissue while natural polymers may degrade too quickly to be used for GTR/GBR [10]. Accordingly, a more attractive approach involves the use of mixtures of natural and synthetic polymers in certain ratios to combine the advantages of both types [11].

In this study, membranes were prepared from PCL or a mixture of PLA/CA. PCL is semi-crystalline, aliphatic polyester [12]. PCL consists of repeating units of one ester group and five methylene groups. Ester bonds are normally degraded in the body. There is no reported evidence showing that PCL induces any cytotoxic effects or accumulate in the body [11,13–15]. PCL composites have been used for fabricating tissue-engineering scaffolds to regenerate bone, ligaments, cartilage, skin, nerve and vascular tissues [12,16,17]. PCL is also suitable candidate for GTR due to its attractive properties as biocompatibility, proper mechanical strength, biodegradability and ease of fabrication [18,19]. However, the use of pure PCL as a scaffold limits the cell adhesion and proliferation which results in poor or slow tissue or bone regeneration. Additionally, the degradation of PCL fibers is usually slower than the desirable rate.

Poly(L-lactic acid) (PLA) has been widely investigated in tissue engineering because of its good biocompatibility [20]. However, the use of the PLA is limited by the poor mechanical properties of the highly porous scaffolds made of the polymer [21]. Moreover, PLA nanofibers interact poorly with cells allowing limited cell migration and adhesion.

In order to combine the advantages of various polymers and overcome their limitations, blends of these polymers are used instead of using a single polymer. The ratio between the constituents of the blends can then be optimized to reach the desired properties. For example, Xue and his coworkers prepared nanofibers from PCL/gelatin mixtures which resulted in improved properties. It was possible to overcome the phase separation between the two polymers by addition of small amount of acetic acid. The nanofibers were also loaded with up to 40% with metronidazole as an antibacterial agent. The use of such formulation can however represent a concern of the allergy towards gelatin. The properties may also differ significantly based on the type of gelatin used [22]. In another study reported by Li et al., PCL was synthesized in a mixture with PLA forming star shaped fiber membranes. PCL provided mechanical strength to the membranes while PLA provided a porous nature to the membrane increasing its surface area. The limitation for such approach is the sensitivity of the resulting membrane morphology towards additives as antibacterial agents or hydroxyapatite [23]. Star-shaped nanoparticles have been prepared with a variety of materials as PbS nanoparticles [24,25]. Bottino and his colleagues reported the preparation of core/shell nanofibers for the same purpose. In their study, PCL was copolymerized with poly(DL-lactide) forming the core of the nanofibers. The core was surrounded with two layers composed of a mixture of the copolymers with PLA and gelatin. The nanofibers were loaded with HANPs to improve the osteoconductivity. Moreover, metronidazole was added to provide antibacterial activity [26]. Mixtures of PLA with cellulose acetate (CA) were also used to prepare GTR/GBR scaffolds. Addition of CA to PLA enhances the cellu-

lar interaction between the scaffolds and cells as fibroblasts [27]. In our previous study, thymoquinone (TQ) was loaded into a mixture of PLA/CA at two different ratios of 7:3 and 9:1 (w/w) to be used as wound dressing. It was found that TQ-loaded PLA/CA at the ratio of 7:3 w/w scaffolds significantly improved the wound healing process [28].

Natural bones consist of hydroxyapatite (HA) embedded in a collagen matrix. Accordingly, a combination of synthetic or natural polymers with a bioactive ceramic can provide enhanced mechanical properties, hydrophilicity, osteoconductivity, osteoinductivity, and/or improved cellular affinities [29,30] Among inorganic bioactive ceramics, hydroxyapatite has been widely investigated as filler. Hydroxyapatite was used with variety of polymers as poly (lactic acid) [31], poly(ε-caprolactone) [32], collagen [33] and gelatin [34]. There are various reported methods for preparation of HANPs. The common idea for most of these methods is the controlled precipitation of hydroxyapatite from its source materials in a non-solvent medium. For example, Cao and his colleagues reported the preparation of needle-shaped nanocrystalline HANPs using ultrasonic irradiation of $Ca(NO_3)_2$ and $NH_4H_2PO_4$ as the source materials. They also showed that increasing the preparation time and temperature increased the yield of the nanoparticles [35]. Sun et al. controlled the morphology of HANPs using reverse microemulsion of water, triton X-100, butanol and cyclohexane. It was also possible to control the nanoparticles using this method by adjusting the pH and the surfactant content [36]. Jarudilokkul and his colleagues prepared amorphous HAPNs using water-in-oil-in-water (W/O/W) emulsion liquid membrane system using Span 20, Tween 80 and caproic acid [37].

Metallic and non-metallic nanoparticles have a wide variety of applications including catalysis and photo-absorption. There is a wide variety of methods reported for the synthesis of nanoparticles including thermal decomposition, flexible ligand method and hydrothermal processes [38–42]. More control over the size of the nanoparticles can be achieved by the synthesis of the nanoparticles in the cavities of other porous materials as zeolite [43].

Since bacterial infections are the main cause for periodontitis, it is common to add antibacterial agents to GTR/GBR scaffolds. For this purpose, silver nanoparticles (AgNPs) can also be used due to their broad spectrum antibacterial activity. AgNPs act by interfering with the cell membrane permeability and transport functions of the bacterial cells. They can also kill the bacterial cells by interacting with sulfur and phosphorus containing molecules as DNA and proteins. Moreover, AgNPs may release Ag^+ ions into the cells which inhibit cellular enzymes and DNA by coordinating to electron rich groups as thiols, hydroxyls, amides and indols [44]. Synthesis of AgNPs has been extensively investigated and there are currently physical, chemical and biological synthesis methods established. Green synthesis of the nanoparticles using plant extracts is preferred approach as it reduces the overall cost, health hazards and impact on the environment upon large scale production. AgNPs were synthesized using plant extracts that can act as reducing and capping agents. There are several reported methods for preparation of AgNPs using various extracts including latex of Jatropha curcas, Capsicum annuum, Azadirachta indica and Ceratonia siliqua extracts [45–48].

The properties of the GTR/GBR scaffolds can differ significantly based on its fabrication and morphology. For example, scaffold porosity is an important parameter affecting tissue regeneration. Scaffolds were previously fabricated in the form of porous foam using conventional techniques as solvent casting, gas foaming or particulate leaching [49,50]. Recently, electrospinning was introduced as a simple and reproducible method for the preparation of thin fibrous membranes [30,51]. The technique can be used for the preparation of fibers with diameters in the range of 3 nm to more than 5 μm [52]. The small diameter of the nanofibers provides huge surface area compared to other types of scaffolds which promote osteoblastic cell function and bone regeneration [53]. Moreover, the pore size of the nanofibers is generally smaller than the cell size thus it can act as a barrier preventing the penetration of connective and epithelial cells [54].

Based on what has been mentioned, we aimed in this study to develop a new series of electrospun nanofibrous scaffolds for GTR/GBR applications. These nanofibers are based on either a combination of polylactic acid and cellulose acetate (PLA/CA) or poly(caprolactone) (PCL) polymers. Additionally, different con-

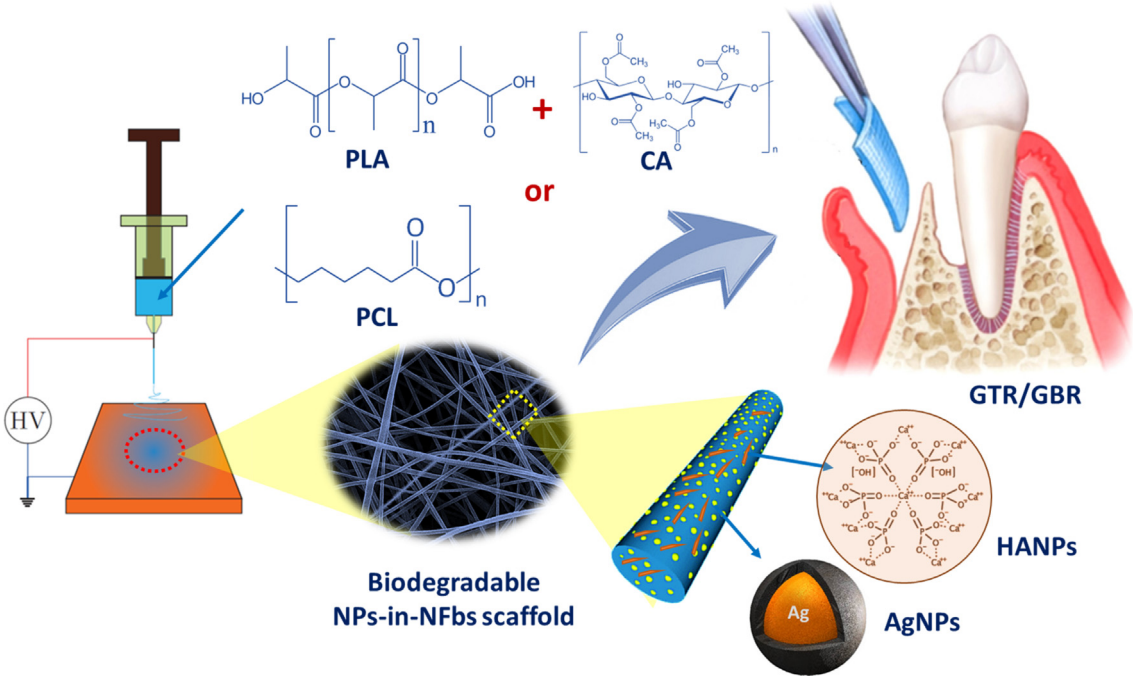

Scheme 1. Development of a new series of electrospun nanoparticles-in-nanofibrous scaffolds for GTR/GBR applications with enhanced antibacterial and bone regeneration activity.

centrations of green-synthesized silver nanoparticles (AgNPs) and hydroxyapatite nanoparticles (HANPs) were incorporated into the scaffolds to enhance their antibacterial and bone regeneration activity (Scheme 1). The developed nanoparticles-in-nanofibrous scaffolds were then evaluated for their physicochemical properties, antibacterial activity, cell viability and tissue regeneration ability. The aim of this approach is to develop simple and efficient GTR/GBR scaffolds that are osteoconductive, biodegradable and antibacterial in addition to having optimal mechanical strength.

Materials and methods

Chitosan (medium molecular weight), 3-(4,5-dimethylthiazolyl-2)-2,5-diphenyltetrazolium bromide (MTT), polycaprolactone (PCL, Mn = 80,000) and silver nitrate (≥99.0%) were purchased from Sigma-Aldrich (Germany). Polylactic acid (PLA) was purchased from Purac (Netherlands). Anhydrous calcium chloride ($CaCl_2$, 98%) was obtained from Oxford Co. (India). Di-ammonium hydrogen orthophosphate ($(NH_4)_2HPO_4$, 33% in H_2O) was purchased from Win Lab, and ammonium solution was provided by Honeywell. All other reagents and solvents were of analytical grade and were used without further purification.

Synthesis of hydroxyapatite nanoparticles (HANPs)

In this study, HANPs were prepared using chemical precipitation method. A solution of 0.16 M $CaCl_2$ was prepared in 20 mL distilled water and the pH was then adjusted to 11 using ammonia solution. Afterwards, 20 mL of 0.1 M $(NH_4)_2HPO_4$ were added dropwise at 40 °C forming a gelatinous precipitate. The mixture was then stirred for 1.5 h. It was then left to age at room temperature for 24 h. The solid product was filtered under vacuum and washed several times with water to remove any residual impurities. The final dry product was obtained by washing several times with ethanol followed by freeze drying [55–57]. Confirmation of the synthesis of HANPs was done using attenuated total reflection Fourier transform infrared (ATR-FTIR) spectroscopy (NECOLET iS10). The crystal structure of the developed nanoparticles (HANPs) was determined using X-ray diffractometer (Bruker Advance D8) while the morphology was investigated using Transmission Electron Microscopy (JEOL TEM-2100) imaging.

Green synthesis of silver nanoparticles (AgNPs)

Various concentrations, durations and temperatures were tested to determine the optimum method for the preparation of AgNPs using *Callistemon viminalis* extract for the first time. In brief, mixtures of 1, 2 and 3 mL of *Callistemon viminalis* extract and 40 mL of aqueous 2 mM $AgNO_3$ were prepared. Mixtures were heated for 1 min, 5 min, 10 min, 20 min, 30 min, 45 min or 60 min at 60 °C, 70 °C, 80 °C or 100 °C. After determination of the optimum conditions for the synthesis of AgNPs, the process was repeated again once with the addition of 1 mL of 3% (w/v) chitosan. The synthesized nanoparticles were then separated by centrifugation at 20,000 rpm for 20 min and the pellet was then washed several times using distilled water followed by freeze drying.

Several characterization methods were used to confirm the synthesis of AgNPs. Reduction of the $AgNO_3$ into AgNPs was monitored using UV–Vis spectrometry (Evolution 600, ThermoScientific, MA, USA). The absorption of the AgNPs suspensions was measured in the range of 200–800 nm using the plant extract as the blank solution. Additionally, the plant extract and the AgNPs solution with the extract were evaluated using FTIR. The morphology and size of the synthesized nanoparticles were investigated using TEM (JEOL TEM-2100) while the crystal structure was determined using X-ray diffraction.

Preparation of nanoparticles-in-nanofibers composites

Electrospinning was used to prepare several nanofibrous composites based on PCL polymer or a mixture of PLA/CA polymers. Both types of nanofibers were prepared with the addition of variable concentrations of HANPs and AgNPs as indicated in Table 1. For preparation of the nanofibers, certain amount of the polymer or polymer mixture was dissolved in a mixture of dichloromethane and dimethylformamide at the ratio of 7:3 (v/v) to obtain a final concentration of 10% (w/v). The solution was kept under stirring for 1–4 h till the complete dissolution of the polymers. Finally, the nanofibers were fabricated using NANO-01A electrospinner (MECC, Japan). The electrospinning parameters were optimized to voltage of 25 kV, feed rate of 2 mL h^{-1}, and distance between the tip of the spinneret and the collector was set to 150 mm.

The morphology of the synthesized nanofibers was examined using scanning electron microscopy (SEM, JEOL-6510LV) at accelerating voltage of 5 kV. The nanofibers were coated using gold sputtering before imaging. The chemical composition of the nanofibers was evaluated using ATR-FTIR. Additionally, the thermal behavior of the prepared nanofibers was examined using differential scanning calorimetry (DSC; Q20, TA Instruments, USA).

Mechanical testing

Tensile strength was measured using Instron Universal Machine (Instron 3345, England). Measurements were done in a 500 N cell at a loading rate of 10 mm/min. Tensile strength was considered as the maximum strength in the stress–strain curve while the tensile modulus was calculated from the initial linear part of the curve [32,58].

Biodegradability and bioactivity testing

Several biological tests were performed to evaluate the biological activity of the prepared nanofibers including biodegradability,

Table 1
Composition, mechanical properties and cell viability assay of the prepared nanofibrous composites.

	Base polymer	HANPs% (w/w)	AgNPs% (w/w)	Tensile stresses at maximum load (MPa)	Tensile modulus (MPa)	Cell Viability %
F1	PCL	–	–	2.77 ± 0.16^{b}	6.60 ± 0.71^{d}	122.27 ± 9.93^{b}
F2	PCL	10	1	3.45 ± 0.15^{a}	20.00 ± 1.51^{b}	150.84 ± 3.37^{a}
F3	PCL	20	1	2.18 ± 0.26^{c}	4.63 ± 0.61^{d}	155 ± 6.88^{a}
F4	PCL	10	2	3.38 ± 0.14^{a}	19.74 ± 0.84^{b}	152.70 ± 6.80^{a}
F5	PLA/CA (7:3)	–	–	2.18 ± 0.19^{c}	13.35 ± 1.08^{c}	116.24 ± 5.63^{b}
F6	PLA/CA (7:3)	10	1	3.39 ± 0.10^{a}	38.37 ± 0.76^{a}	141.48 ± 5.45^{a}
F7	PLA/CA (7:3)	20	1	2.22 ± 0.15^{c}	23.28 ± 1.46^{b}	142.86 ± 2.29^{a}
F8	PLA/CA (7:3)	10	2	3.13 ± 0.28^{ab}	37.49 ± 2.20^{a}	151.80 ± 1.96^{a}

Means with the same superscript letter are not significantly different ($p < 0.05$).

antibacterial activity and *in-vitro* cellular response. Biodegradability of the nanofibers was evaluated using gravimetric method. Nanofibrous films were cut into 10 × 10 mm^2 samples for assessment of biodegradability and water adsorption. Weight of the cut samples were recorded (W_0). Samples were then placed in 5 mL of simulated body fluid (SBF) at 37 °C in an orbital shaker incubator for 1, 2, 4 and 8 weeks. The SBF was replaced with fresh 5 mL every week. At the specified time intervals, samples were removed from the fluid and the water was removed from the surface using filter papers, and the weight of the sample was recorded at this point (W_1). The dry weight of the samples (W_2) was recorded after drying of the samples using freeze-drying. The percentage of weight loss (L) was calculated using the following equation [59]

$$L = \frac{(W2 - W0)}{W0} \times 100$$

The rate of water absorption (A) was determined using the following equation:

$$A = \frac{(W1 - W2)}{W2} \times 100$$

Deformations in the surface morphology of the nanofibers were examined using SEM imaging. Additionally, the release profile of the calcium against time in the SBF fluids was measured using atomic absorption spectrophotometer (AA-7000/GFA-7000/ASC-7000, Shimadzu, Japan). The concentration of Ag released at different time intervals was also monitored and then calculated using the following equation:

$$C_n = C_{n\ means} + A/V \sum_{(s=1)}^{(n-1)} \cdot Cs\,means$$

where C_n is the expected n^{th} sample concentration, $C_{n\ means}$ is the measured concentration, A is the volume of withdrawn aliquot, V is the volume of the dissolution medium, n^{-1} is the total volume of all the previously withdrawn samples before the currently measured sample, and Cs is the total concentration of all previously measured samples before the currently measured sample.

Release study of AgNPs and antibacterial activity

Release of AgNPs from the nanofibers was assessed using atomic absorption spectroscopy. Briefly, parts of the nanofibers with specific dimensions were incubated in 5 mL of PBS at pH 7.4 with the temperature set to 37 °C and rotation speed 70 rpm. Certain volume of the medium was withdrawn after 1, 2, 4, 8, 16, and 32 days for measurement of AgNPs concentration using atomic absorption spectroscopy. The volume withdrawn was replaced by fresh buffer to maintain the volume constant [60,61].

Antibacterial activity was measured in terms of inhibition zones. Briefly, 1 mL of the previously withdrawn solutions for the release profile was added to 10 mm diameter holes cut into agar gel containing gram negative bacteria (Escherichia coli ATCC 25922) or gram positive bacteria (*Enterococcus faecalis* ATCC 29212) at a bacterial concentration of 10^8 cells/mL. Plates were then incubated for 24 h at 37 °C [62].

Cytotoxicity assay

The cytotoxicity of the prepared nanofibers was evaluated using MTT assay. The PCL and PLA/CA nanofibers were placed in a 24-well plate and seeded with 10 × 10^5 cells which were then incubated for 3 days at 37 °C. The MTT assay was performed following the standard procedures reported in previous studies [63].

Statistical analysis

Means and standard deviations were calculated for each group. The data were analyzed using one-way and two-way ANOVA followed by post-hoc test for determining significant differences among different groups at $p = 0.05$ level. The statistical analysis was performed by Statistical Package for Social Science (SPSS) version 23.

Results

Silver nanoparticles, hydroxyapatite nanoparticles and nanofibrous composites

Results for characterization of the green-synthesized AgNPs, HANPs and the nanofibrous composites are shown in the supplementary data (Figs. S1–S5).

Mechanical characterization

It was found that the addition of 10% HANPs has significantly increased ($P < 0.05$) the tensile strength of both PCL and PLA/CA nanofibers. Interestingly, higher increase in the concentration of the HANPs up to 20% resulted in a significant decrease ($P < 0.05$) of the tensile strength. Table 1 shows the results for the tensile strength and tensile modulus for all the prepared nanofibers.

Biodegradability assessment

The biodegradation of the nanofibers was evaluated using SEM imaging and in terms of weight loss and water absorption after soaking of the nanofibers in SBF for 2 or 8 weeks as shown in Figs. 1 and 2. Precipitation of CaP was not observed after 2 weeks of soaking the plain nanofibers (PCL or PLA/CA) in SBF solutions, however, after 8 weeks the surface of PCL nanofibers was coated with CaP while the precipitation of CaP was observed as agglomerates surrounding the PLA/CA nanofibers. Presence of 10% and 20% HANPs resulted in obvious precipitation of CaP after 2 weeks and a higher increase after 8 weeks where all the nanofibers were completely covered by a layer of nano-textured cauliflower-like coatings. The total amount of Ca deposited on the nanofibers was calculated as the difference between the initial Ca concentration in SBF and the remaining concentration after the soaking period which was measured using atomic absorption spectrophotometer (AA-7000/GFA-7000/ASC-7000, Shimadzu, Japan). It was also obvious that Ca deposition increases with increasing the soaking time.

Moreover, the obtained results indicated a significant effect ($P < 0.001$) of the composition of the nanofibrous membrane and time of immersion on both the weight loss and water absorption. It was found that addition of 10% HANPs (F2, F4, F6 and F8) resulted in a significant reduction in the biodegradation rate compared to the blank PCL (F1) and PLA/CA (F5) nanofibers. This biodegradation rate of the nanofibers was further retarded upon incorporation of 20% HANPs (F3 and F7). A comparison for the rate of weight loss and water absorption for all the tested nanofibers is shown in Fig. 3.

Bioactivity assessment

Silver ions release

The release profiles of AgNPs from the prepared nanofibers are shown in Fig. 4. It was found that all prepared fibers were able to sustain the release of the loaded AgNPs for more than 35 days. It was also found that the formula F4 and F8 which contain 10% HANPs and 2% AgNPs have the highest release rate compared to

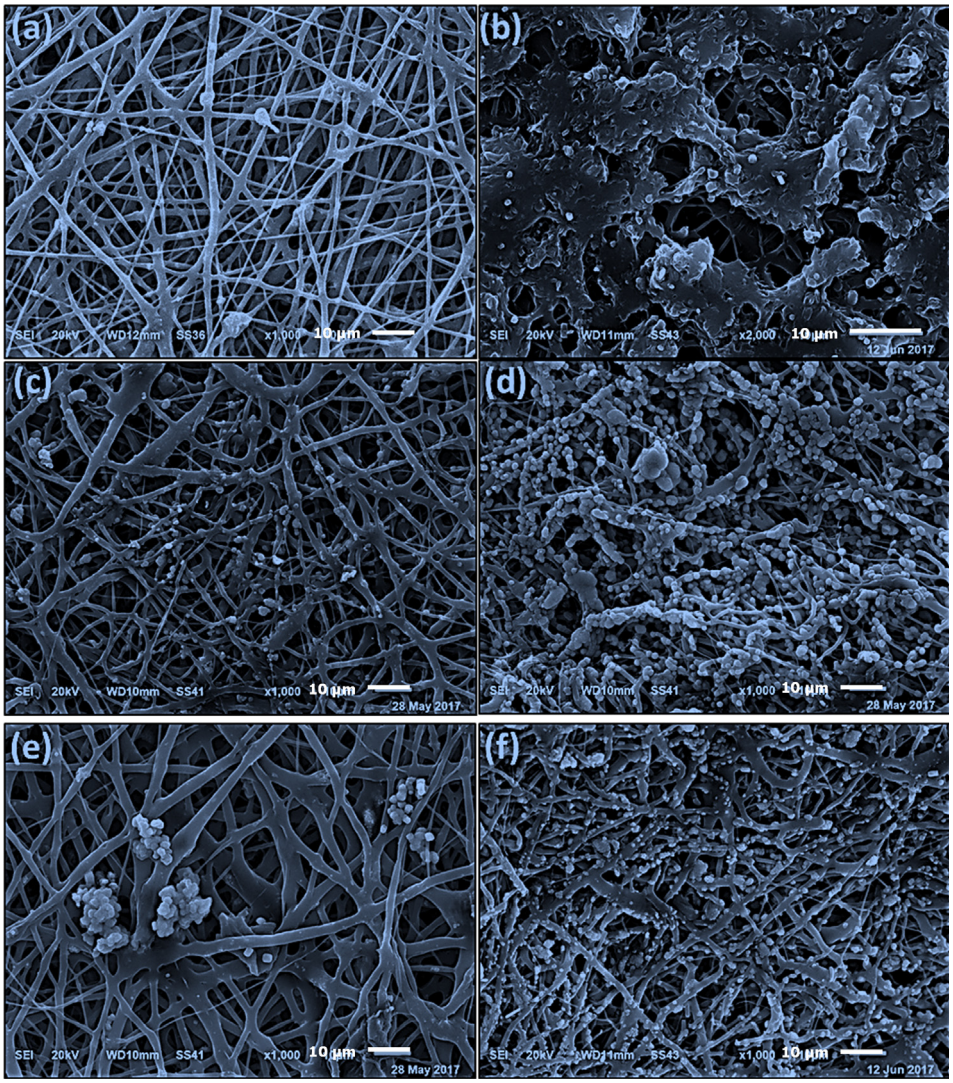

Fig. 1. SEM micrographs of the developed PCL nanofibers after immersion in SBF for 2 and 8 weeks, respectively. (a, b) PCL, (c, d) PCL with 10% HANPs and 2% AgNPs and (e, f) PCL with 20% HANPs and 1% AgNPs.

the remaining nanofibers. The pattern of these two formulations showed an initial burst release followed by a steady release at almost the same rate as other formulations.

Antibacterial activity

The antibacterial activity of the solutions withdrawn at 8, 16 and 32 days in PBS was tested against *Enterococcus faecalis* (Gram-positive) and *Escherichia coli* (Gram-negative). Results of the antibacterial assay are summarized in Fig. 5. A significant interaction between the nanofibrous membrane materials and time ($P < 0.001$) was noted against *Enterococcus faecalis* and *Escherichia coli*.

All the fibers loaded with AgNPs showed the ability to inhibit the growth of both bacterial strains while blank nanofibers (F1 and F5) did not show any antibacterial activity. Moreover, increasing the concentration of AgNPs significantly increased the antibacterial activity. It was also noticed that the inhibition zones were larger against *E. faecalis* compared to that against *E. coli* and that the inhibitory effect increases with increasing time.

In vitro cellular response

The results for cell viability assay are summarized in Table 1. It can be noted that both PLA/CA and PCL nanofibers supported the growth of bone marrow stromal cells (BMSCs) without any significant cytotoxicity. It was also found that PCL nanofibers increased the cell viability by 22% compared to the control at day 3 while PLA/CA nanofibers increased the viability by 16%. Addition of HANPs provided further increase in the viability as the PCL nanofibers and PLA/CA nanofibers loaded with HANPs increased the viability by 50–55% and 41–51%, respectively, and there was no significant difference between the nanofibers loaded with 10% and 20% HANPs.

Discussion

The reconstruction of large tissue defects still represents unsolved challenge facing the surgical community. These large defects may occur in the oral cavity as a result of trauma, tumor resection or periodontal infection. Accordingly, several regeneration methods were developed to rehabilitate such cases. The most commonly accepted methods for such purpose are GTR and GBR which are used together to regenerate various periodontal tissues including alveolar bone, cementum, PDL, and gingiva [64–67]. GBR is also used frequently before placement of dental implants for the augmentation of deficient ridges with decreased bone

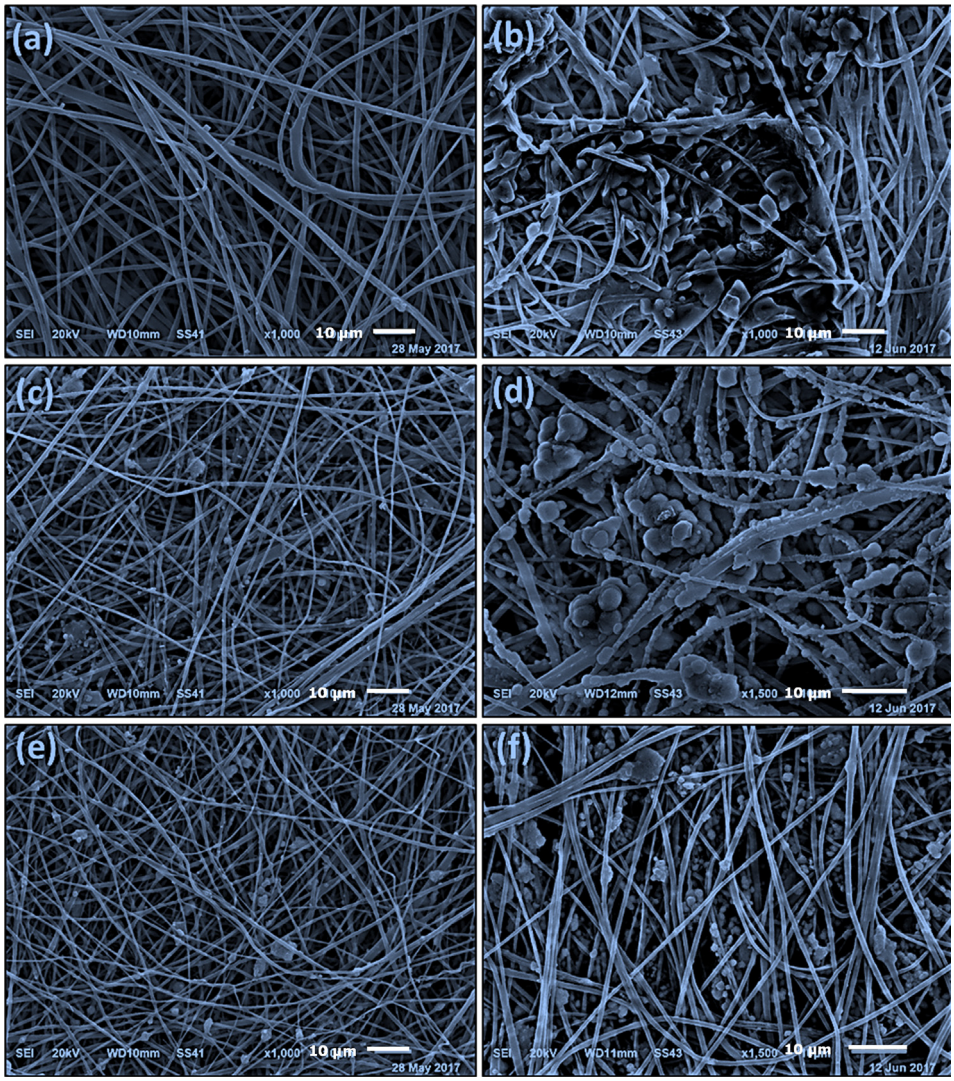

Fig. 2. SEM micrographs of PLA/CA-based nanofibers after immersion in SBF for 2 and 8 weeks, respectively. (a, b) PLA/CA, (c, d) PLA/CA with 10% HANPs and 2% AgNPs and (e, f) PLA/CA with 20% HANPs and 1% AgNPs.

height. In these techniques, an occlusive membrane is used at the interface between the gingival connective tissue/epithelium and periodontal ligament PDL/ alveolar bone tissues. This aims at maintaining the space for clot stabilization and promoting periodontal tissue regeneration, while preventing postsurgical epithelial cell migration to the wound site. These procedures provide the opportunity for certain cell populations residing in periodontal tissues to populate the periodontal wound or defect and reverse periodontal destruction.

Non-biodegradable membranes were used previously which required a second surgery for removal. However, the introduction of new resorbable materials has eliminated the need for a second surgery [68,69]. These materials are mainly polymers that are used with other additives to either enhance the antibacterial activity or stimulate bone deposition [70,71]. Beforehand, traditional methods were used for the preparation of such materials as particulate leaching, solvent casting or gas foaming. Currently, electrospinning could be used for this purpose which allows the preparation of thin fibrous membranes [53]. We report in the present study, the development of a new series of GTR/GBR nanoparticles-in-nanofibrous membranes using electrospinning. The nanofibrous membranes were based on PCL and PLA/CA polymers with the addition of green-synthesized AgNPs and HANPs to improve the antimicrobial activity, and the osteo-conductivity as well as the bone-bonding ability, respectively.

Synthesis and characterization of HANPs and AgNPs

Hydroxyapatite is water-insoluble Ca mineral with the chemical formula $Ca_5(PO_4)_3(OH)$. Carbonated hydroxyapatite is the major constituent of human bones representing around 50% of the bone volume and around 70% of its mass [72]. HANPs were synthesized in this study using chemical precipitation which depends on mixing the water soluble reactants to yield an insoluble product that precipitates in a controlled manner. The morphology and crystal structure of the resulting nanoparticles are controlled by the reaction temperature and time. These factors have been extensively investigated in previously reported studies [55–57]. HANPs have been successfully synthesized as confirmed using XRD and FTIR. The XRD pattern showed peaks that are only characteristic to hydroxyapatite. Also, FTIR spectra confirmed the formation of apatite phase containing CO_2^{3-} as indicated by the presence of the peak at 869 cm^{-1}. Carbonated hydroxyapatite resembles the hydroxyapatite present in the mineral phase of natural dentin [73].

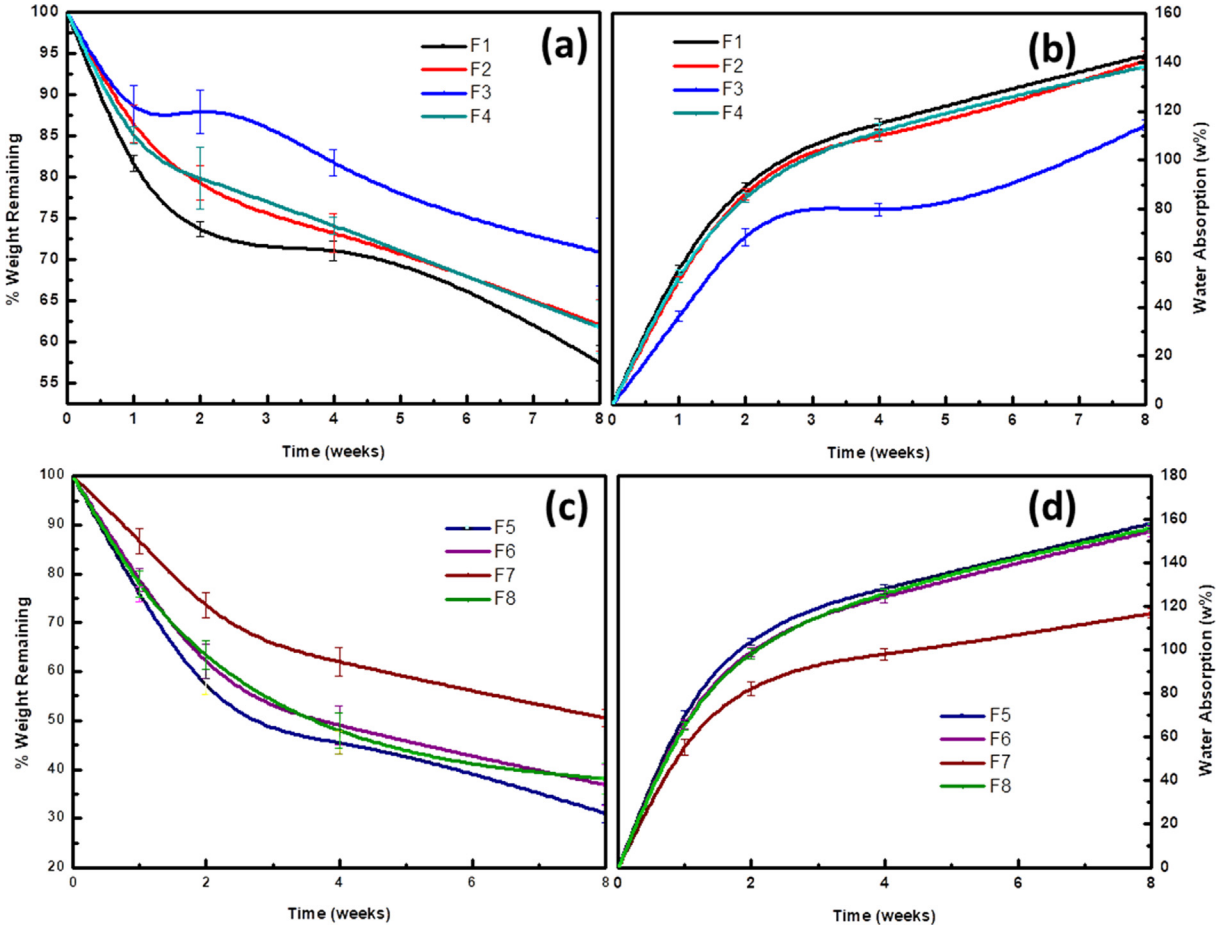

Fig. 3. Rate of biodegradation (measured as weight loss) and water absorption of the developed nanofibers after immersion in SBF for 8 weeks.

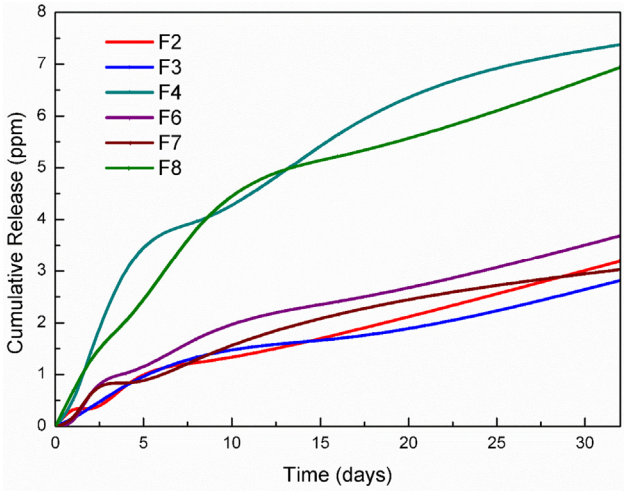

Fig. 4. Release profiles of Ag^+ from the electrospun nanofibers composites in PBS.

Green-synthesis of AgNPs has been achieved using various concentrations of an aqueous *Callistemon viminalis* extract and chitosan with heating. The extract is rich in flavonoids and polyphenols that are responsible for the reduction of Ag^+ to the Ag^0 [74]. The formation and stability of the nanoparticles was confirmed using UV–Visible spectrophotometry. The peak appearing at 420–440 nm for the AgNPs results from the coherent oscillation of the surface electrons (surface plasmon resonance). It was observed that adding 1 mL of the extract using the reported method is the optimum amount for the synthesis. Higher concentration of the extract was detrimental to the concentration of the AgNPs formed as indicated by the peak intensity. This may be attributed to the fast reduction of the Ag^+ ions that may result in uncontrolled growth of the nanoparticles. Additionally, it was observed that the intensity of the peak increased by increasing the heating temperature to 100 °C for a time period up to 45 min which might be related to the concentration, size and shape of the formed AgNPs. It was also observed that the addition of chitosan resulted in increasing the intensity of the peak. This can be attributed to the ability of chitosan to chelate Ag^+ by the OH and NH_2 groups of the β (1–4) d-glucosamine units. Additionally, chitosan acts as a stabilizer for the formed AgNPs preventing its aggregation at the macroscopic level due to the ion–dipole intermolecular forces [75]. It was also obvious from the XRD pattern that the synthesized nanoparticles have crystalline nature. In addition, FTIR was used to investigate the presence of reducing and stabilizing biomolecules in the *Callistemon viminalis* extract. The strong broad band that appeared at around 3240 cm^{-1} suggests the presence of –OH groups which are responsible for the reduction of Ag^+ into Ag^0 and accordingly forming the nanoparticles.

Fabrication and characterization of the nanofibers

Physicochemical characterization

Electrospinning was used for the preparation of the nanofibers from PCL or PLA/CA polymers with the addition of HANPs or AgNPs.

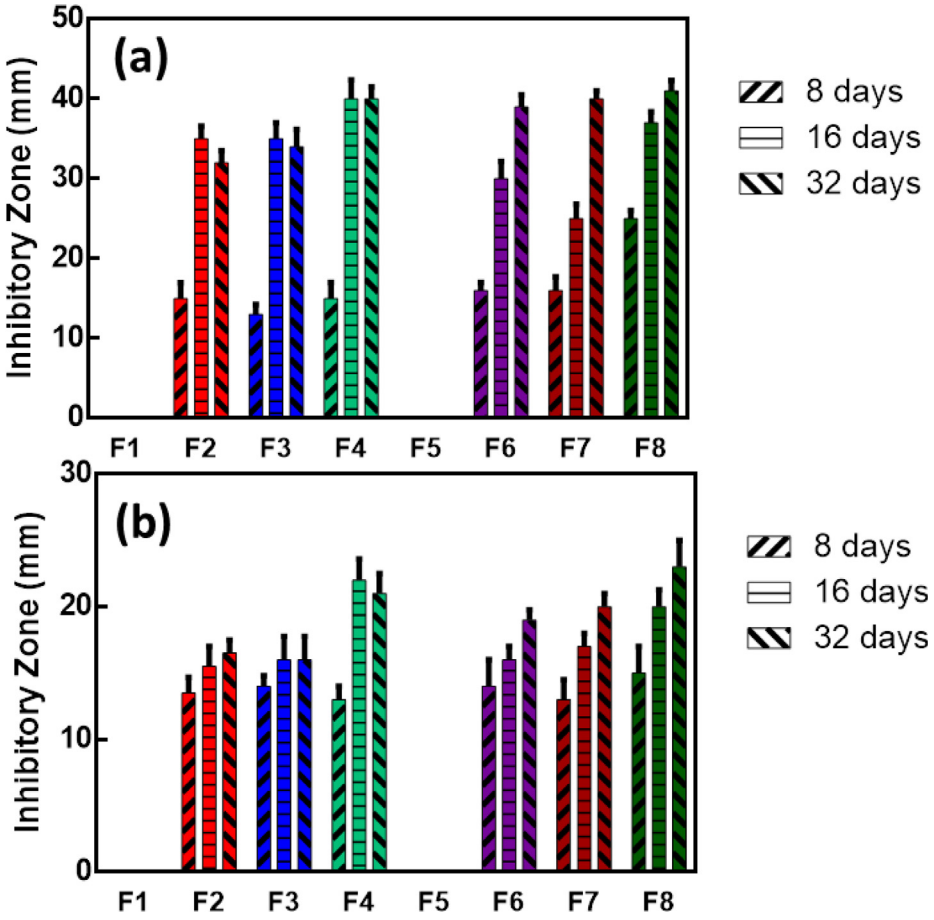

Fig. 5. Mean and standard deviations of inhibition zones (mm) against (a) *E. faecalis* and (b) *E. Coli.*

Although it was preferred to use DCM as a volatile solvent that results in the formation of uniform fibers, DMF was added to improve the dissolution and dispersion of the polymers and nanoparticles. The optimum ratio between DCM and DMF was found to be 7:3 which allowed the homogenous distribution of materials and the preparation of uniform nanofibers. SEM confirmed the formation of submicron nanofibers with the nanoparticles uniformly distributed within these fibers. The nanofibrous structure resulted in a high surface area-to-volume ratio and high interconnected porosity. These characteristics are essential for efficient nutrient and oxygen delivery to the cells and accordingly promoting cellular growth [76].

Bioactivity tests and biodegradation

The bone forming ability of the prepared nanofibers was the main desired characteristic in this study. It was evaluated by incubating the nanofibers in SBF containing the same ionic concentrations as the human plasma and measuring their ability to form apatite on its surface after specific period of time [77]. The apatite is not normally formed on synthetic polymers without activation of its surfaces. This was also evident in this study as the blank PCL and PLA/CA nanofibers did not show any apatite after incubation for 2 weeks as shown in Figs. 1 and 2. However, addition of HANPs promoted the precipitation of apatite on the nanofibers. The effect of the HANPs can be attributed to 2 factors: (a) dissolution of the nanoparticles and subsequent release of its calcium content and (b) presence of the nanoparticles on the surface act as nucleation site for apatite formation and growth [78,79].

The in-vitro biodegradation assay showed that the weights of all the nanofibers were continuously decreasing indicating their degradation. Addition of HANPs resulted in decreasing the rate of degradation which was more obvious with fibers containing 20 w% HANPs. This can be explained based on the nature of the synthesized nanofibers. PLA is a biodegradable polymer with repeating ester bonds that are hydrolyzed randomly in aqueous medium as the SBF with pH 7.4. Hydrolysis results in generation of carboxylic groups which in turn accelerate the hydrolysis process by autocatalysis. Incorporation of HANPs slows down the degradation as the dissolution of these alkaline nanoparticles results in inhibiting the autocatalysis process and blocking the entry of water molecules [34,80].

Mechanical testing

In surgery, the GBR/GTR membranes must be tightly fixed using biodegradable sutures, pins or medical glue to prevent them from sagging into bone defects. Accordingly, it is necessary to test the mechanical properties of the prepared nanofibers to ensure that it is suitable for the intended purpose. Mechanical testing showed that the addition of 10% of HANPs to the nanofibers resulted in increasing the tensile strength and modulus of both PCL and PLA/CA nanofibrous membranes. This can be attributed to the additional energy dissipating effect of the nanoparticles. Recent molecular dynamics studies proposed that this effect is attributed to the mobility of the nanoparticles which orient and align under tensile strength. Temporary crosslinks are then formed between the polymer chains creating local areas of enhanced strength. The increase in the tensile modulus may result from the increased rigidity compared to the pure polymer nanofibers along with the strong adhesion between the two materials [81].

On the contrary, further increase in the concentration of HANPs resulted in a significant reduction in the tensile strength and modulus of both PCL and PLA/CA nanofibers. This brittle nature can be attributed to the stacking of the nanoparticles which results in increasing their size and decreasing mobility. Accordingly, the energy dissipating effect is lost which is consistent with the previously reported results [82].

Antibacterial testing of the developed nanofibrous membranes

The prepared nanofibers showed the ability to maintain a steady and prolonged release of AgNPs with the accumulative release amount of silver ions reaching 2.82–3.69 ppm for nanofibrous membranes containing 1% AgNPs and 6.94–7.38 ppm for the membranes containing 2% AgNPs. It should be noted that the threshold concentration for the antibacterial activity of AgNPs is 0.1 ppm which suggests that the prepared nanofibrous membranes would have a significant antibacterial effect [83].

Testing of the AgNPs-loaded nanofibers showed their ability to inhibit the growth of *Enterococcus faecalis* and *Escherichia coli* for 32 days, however, the inhibitory activity was relatively lower towards *E. coli* compared to the inhibition of *E. faecalis* growth which is in alignment with the results of a previous study [60]. This is probably caused by the different composition of the cell wall in gram negative and gram positive bacteria. The cell wall of *E. coli* contains lipids, proteins and lipopolysaccharides (LPS) and is effective in protecting the bacterial cells from biocides. The cell wall of *E. faecalis*, in turn does not contain LPS [84]. It was also noted that the inhibitory activity of the nanofibers increased by time with the highest activity observed after 32 days. This is mainly attributed to the degradation of the nanofibers and the availability of higher concentrations of the AgNPs.

The exact mechanism of the antibacterial activity of AgNPs is still not clear. Three mechanisms for this action have been proposed by Feng et al. Firstly, AgNPs attach to the surface of the bacterial cells disrupting the power functions as respiration and permeability. This effect is directly related to the surface area of the AgNPs which increases by decreasing the size. Additionally, AgNPs can penetrate into the cells and cause damage by interacting with sulfur and phosphorus-containing molecules as DNA. Finally, the nanoparticles release Ag^+ ions which also contribute to the bactericidal effect. Silver ions inhibit DNA replication ability and inactivate cellular proteins. Besides, the higher concentrations of Ag^+ ions interfere with the function of cytoplasmic components and nucleic acids [85–90].

Cell viability assay

The measurement of cell viability using MTT assay depends on the reduction of yellow tetrazolium to purple formazan by mitochondrial dehydrogenase enzyme present in viable cells. Accordingly, the intensity of the purple color of formazan, measured using UV–Vis spectrophotometry, is directly proportional to the amount of dehydrogenase enzyme which is in turn indicative of the cell viability. It should be taken into consideration that reduction in the metabolic activity is considered as early signs for cellular damage and reduced cell viability.

In this study we used mesenchymal stem cells which are self-renewing multipotent cells that function to repair various tissues in response to injury. These cells play a major role in maintaining the stem cell niche and tissue homeostasis. They are particularly suitable for *in-vitro* studies due to their ability to withstand freezing and the high replication capacity [91–93]. The *in-vitro* cell viability assay showed that all prepared nanofibers were cytocompatible and that the addition of HANPs improved the cytocompatibility by maintaining cells viable and supporting their proliferation. The effect of HANPs can be attributed to the coarse surface created by the addition of the nanoparticles which increases the actual contact area. Additionally, the particles provide the nanotopography that stimulates the cell adhesion and proliferation [94]. Moreover, the HANPs that disengage from the fibers and dissolve in the body fluids can induce changes in the microenvironment by increasing its pH which results in positive effects on cell metabolism [95].

Conclusion

In this study we reported the preparation of a new series of nanoparticles-in-nanofibers scaffolds for guided periodontal tissue and bone regeneration with enhanced antibacterial activity. The nanofibrous scaffolds were prepared from PCL or PLA/CA at the ratio of 7:3. Preparation was done using electrospinning with the addition of various concentrations (0%, 10% or 20% w/w) of HANPs, and (0%, 1% or 2% w/w) of AgNPs. Results depicted that the nanofibers had prominent properties to be used for GTR/GBR applications as indicated by their ability to enhance the cell viability by about 50% and to provide sustained antibacterial activity for 32 days. Besides, the nanofibers have demonstrated optimum mechanical properties with the tensile modulus reaching around 20 and 38 MPa for PCL and PLA/CA nanofibers, respectively. The nanofibers degraded slowly in SBF losing 30–40% of their weight in 8 weeks for the PCL-based nanofibers and around 40–70% for the PLA/CA nanofibers. We also focused on using green, simple and reproducible methods for preparation of the nanoparticles and the nanofibers. The prepared scaffolds loaded with HANPs were able to promote the formation of apatite and the proliferation of mesenchymal stem cells *in-vitro* which predicts enhanced bone formation *in-vivo*. Future studies should include *in-vivo* testing of the developed nanoparticles-in-nanofibers membranes.

Funding

No funding was received to support the current study.

Declaration of Competing Interest

The authors declare that they have no known competing financial interests or personal relationships that could have appeared to influence the work reported in this paper.

Appendix A. Supplementary material

Supplementary data to this article can be found online at https://doi.org/10.1016/j.jare.2020.06.014.

References

[1] Haffajee AD, Socransky SS. Microbial etiological agents of destructive periodontal diseases. Periodontology 1994;2000. doi: https://doi.org/10.1111/j.1600-0757.1994.tb00020.x.
[2] Piattelli A, Scarano A, Russo P, Matarasso S. Evaluation of guided bone regeneration in rabbit tibia using bioresorbable and non-resorbable membranes. Biomaterials 1996. doi: https://doi.org/10.1016/0142-9612(96)81416-5.
[3] Nickles K, Ratka-Krüger P, Neukranz E, Raetzke P, Eickholz P. Open flap debridement and guided tissue regeneration after 10 years in infrabony defects. J Clin Periodontol 2009. doi: https://doi.org/10.1111/j.1600-051X.2009.01474.x.
[4] Retzepi M, Donos N. Guided bone regeneration: biological principle and therapeutic applications. Clin Oral Implant Res 2010. doi: https://doi.org/10.1111/j.1600-0501.2010.01922.x.
[5] Gotfredsen K, Nimb L, Hjørting-hansen E. Immediate implant placement using a biodegradable barrier, polyhydroxybutyrate-hydroxyvalerate reinforced with polyglactin 910. An experimental study in dogs. Clin Oral Implant Res 1994. doi: https://doi.org/10.1034/j.1600-0501.1994.050204.x.
[6] Murphy WL, Kohn DH, Mooney DJ. Growth of continuous bonelike mineral within porous poly(lactide-co- glycolide) scaffolds in vitro. J Biomed Mater Res

2000. doi: https://doi.org/10.1002/(SICI)1097-4636(200004)50:1<50::AID-JBM8>3.0.CO;2-F.
[7] Selvig KA, Nilveus RE, Fitzmorris L, Kersten B, Khorsandi SS. Scanning electron microscopic observations of cell population and bacterial contamination of membranes used for guided periodontal tissue regeneration in humans. J Periodontol 1990. doi: https://doi.org/10.1902/jop.1990.61.8.515.
[8] Mano JF, Silva GA, Azevedo HS, Malafaya PB, Sousa RA, Silva SS, et al. Natural origin biodegradable systems in tissue engineering and regenerative medicine: Present status and some moving trends. J R Soc Interface 2007. doi: https://doi.org/10.1098/rsif.2007.0220.
[9] Nair LS, Laurencin CT. Biodegradable polymers as biomaterials. Progr Polym Sci (Oxf) 2007. doi: https://doi.org/10.1016/j.progpolymsci.2007.05.017.
[10] Jose MV, Thomas V, Johnson KT, Dean DR, Nyairo E. Aligned PLGA/HA nanofibrous nanocomposite scaffolds for bone tissue engineering. Acta Biomater 2009. doi: https://doi.org/10.1016/j.actbio.2008.07.019.
[11] Shi R, Xue J, He M, Chen D, Zhang L, Tian W. Structure, physical properties, biocompatibility and in vitro/vivo degradation behavior of anti-infective polycaprolactone-based electrospun membranes for guided tissue/bone regeneration. Polym Degrad Stab 2014. doi: https://doi.org/10.1016/j.polymdegradstab.2014.07.017.
[12] Ulery BD, Nair LS, Laurencin CT. Biomedical applications of biodegradable polymers. J Polym Sci Part B: Polym Phys 2011. doi: https://doi.org/10.1002/polb.22259.
[13] Woodruff MA, Hutmacher DW. The return of a forgotten polymer - Polycaprolactone in the 21st century. Progr Polym Sci (Oxf) 2010. doi: https://doi.org/10.1016/j.progpolymsci.2010.04.002.
[14] Lo HY, Kuo HT, Huang YY. Application of polycaprolactone as an anti-adhesion biomaterial film. Artif Organs 2010. doi: https://doi.org/10.1111/j.1525-1594.2009.00949.x.
[15] Huynh NCN, Everts V, Nifuji A, Pavasant P, Ampornaramveth RS. Histone deacetylase inhibition enhances in-vivo bone regeneration induced by human periodontal ligament cells. Bone 2017. doi: https://doi.org/10.1016/j.bone.2016.11.017.
[16] Chuenjitkuntaworn B, Osathanon T, Nowwarote N, Supaphol P, Pavasant P. The efficacy of polycaprolactone/hydroxyapatite scaffold in combination with mesenchymal stem cells for bone tissue engineering. J Biomed Mater Res – Part A 2016. doi: https://doi.org/10.1002/jbm.a.35558.
[17] Osathanon T, Chuenjitkuntaworn B, Nowwarote N, Supaphol P, Sastravaha P, Subbalekha K, et al. The responses of human adipose-derived mesenchymal stem cells on polycaprolactone-based scaffolds: an in vitro study. Tissue Eng Regener Med 2014;11:239–46.
[18] Fecek C, Yao D, Kaçorri A, Vasquez A, Iqbal S, Sheikh H, et al. Chondrogenic derivatives of embryonic stem cells seeded into 3D polycaprolactone scaffolds generated cartilage tissue in vivo. Tissue Eng – Part A 2008. doi: https://doi.org/10.1089/ten.tea.2007.0293.
[19] Li WJ, Jiang YJ, Tuan RS. Cell-nanofiber-based cartilage tissue engineering using improved cell seeding, growth factor, and bioreactor technologies. Tissue Eng – Part A 2008. doi: https://doi.org/10.1089/tea.2007.0136.
[20] Montjovent MO, Mathieu L, Hinz B, Applegate LL, Bourban PE, Zambelli PY, et al. Biocompatibility of bioresorbable poly(L-lactic acid) composite scaffolds obtained by supercritical gas foaming with human fetal bone cells. Tissue Eng 2005. doi: https://doi.org/10.1089/ten.2005.11.1640.
[21] Zhang R, Ma PX. Poly(α-hydroxyl acids)/hydroxyapatite porous composites for bone- tissue engineering. I. Preparation and morphology. J Biomed Mater Res 1999. doi: https://doi.org/10.1002/(SICI)1097-4636(19990315)44:4<446::AID-JBM11>3.0.CO;2-F.
[22] Xue J, He M, Liu H, Niu Y, Crawford A, Coates PD, et al. Drug loaded homogeneous electrospun PCL/gelatin hybrid nanofiber structures for anti-infective tissue regeneration membranes. Biomaterials 2014. doi: https://doi.org/10.1016/j.biomaterials.2014.07.060.
[23] Li H, Qiao T, Song P, Guo H, Song X, Zhang B, et al. Star-shaped PCL/PLLA blended fiber membrane via electrospinning. J Biomater Sci Polym Ed 2015. doi: https://doi.org/10.1080/09205063.2015.1015865.
[24] Salavati-Niasari M, Ghanbari D, Loghman-Estarki MR. Star-shaped PbS nanocrystals prepared by hydrothermal process in the presence of thioglycolic acid. Polyhedron 2012. doi: https://doi.org/10.1016/j.poly.2012.01.010.
[25] Salavati-Niasari M, Sobhani A, Davar F. Synthesis of star-shaped PbS nanocrystals using single-source precursor. J Alloys Compd 2010. doi: https://doi.org/10.1016/j.jallcom.2010.06.062.
[26] Bottino MC, Thomas V, Janowski GM. A novel spatially designed and functionally graded electrospun membrane for periodontal regeneration. Acta Biomater 2011. doi: https://doi.org/10.1016/j.actbio.2010.08.019.
[27] Fischer S, Thümmler K, Volkert B, Hettrich K, Schmidt I, Fischer K. Properties and applications of cellulose acetate. Macromol Symp 2008. doi: https://doi.org/10.1002/masy.200850210.
[28] Gomaa SF, Madkour TM, Moghannem S, El-Sherbiny IM. New polylactic acid/cellulose acetate-based antimicrobial interactive single dose nanofibrous wound dressing mats. Int J Biol Macromol 2017. doi: https://doi.org/10.1016/j.ijbiomac.2017.07.145.
[29] Webster TJ, Ergun C, Doremus RH, Siegel RW, Bizios R. Specific proteins mediate enhanced osteoblast adhesion on nanophase ceramics. J Biomed Mater Res 2000. doi: https://doi.org/10.1002/1097-4636(20000905)51:3<475::AID-JBM23>3.0.CO;2-9.
[30] Fujihara K, Kotaki M, Ramakrishna S. Guided bone regeneration membrane made of polycaprolactone/calcium carbonate composite nano-fibers. Biomaterials 2005. doi: https://doi.org/10.1016/j.biomaterials.2004.09.014.
[31] Sonseca A, Peponi L, Sahuquillo O, Kenny JM, Giménez E. Electrospinning of biodegradable polylactide/hydroxyapatite nanofibers: study on the morphology, crystallinity structure and thermal stability. Polym Degrad Stab 2012;97:2052–9.
[32] Yang F, Both SK, Yang X, Walboomers XF, Jansen JA. Development of an electrospun nano-apatite/PCL composite membrane for GTR/GBR application. Acta Biomater 2009;5:3295–304.
[33] Thomas V, Dean DR, Jose MV, Mathew B, Chowdhury S, Vohra YK. Nanostructured biocomposite scaffolds based on collagen coelectrospun with nanohydroxyapatite. Biomacromolecules 2007. doi: https://doi.org/10.1021/bm060879w.
[34] Kim HW, Song JH, Kim HE. Nanofiber generation of gelatin-hydroxyapatite biomimetics for guided tissue regeneration. Adv Funct Mater 2005. doi: https://doi.org/10.1002/adfm.200500116.
[35] Cao LY, Zhang CB, Huang JF. Synthesis of hydroxyapatite nanoparticles in ultrasonic precipitation. Ceram Int 2005. doi: https://doi.org/10.1016/j.ceramint.2004.11.002.
[36] Sun Y, Guo G, Tao D, Wang Z. Reverse microemulsion-directed synthesis of hydroxyapatite nanoparticles under hydrothermal conditions. J Phys Chem Solids 2007. doi: https://doi.org/10.1016/j.jpcs.2006.11.026.
[37] Jarudilokkul S, Tanthapanichakoon W, Boonamnuayvittaya V. Synthesis of hydroxyapatite nanoparticles using an emulsion liquid membrane system. Colloids Surf, A 2007. doi: https://doi.org/10.1016/j.colsurfa.2006.09.038.
[38] Davar F, Salavati-Niasari M, Mir N, Saberyan K, Monemzadeh M, Ahmadi E. Thermal decomposition route for synthesis of Mn3O4 nanoparticles in presence of a novel precursor. Polyhedron 2010. doi: https://doi.org/10.1016/j.poly.2010.02.026.
[39] Salavati-Niasari M. Ship-in-a-bottle synthesis, characterization and catalytic oxidation of styrene by host (nanopores of zeolite-Y)/guest ([bis (2-hydroxyanil) acetylacetonato manganese (III)]) nanocomposite materials (HGNM). Microporous Mesoporous Mater 2006;95:248–56.
[40] Sabet M, Salavati-Niasari M, Amiri O. Using different chemical methods for deposition of CdS on TiO2 surface and investigation of their influences on the dye-sensitized solar cell performance. Electrochim Acta 2014. doi: https://doi.org/10.1016/j.electacta.2013.11.176.
[41] Mohandes F, Davar F, Salavati-Niasari M. Magnesium oxide nanocrystals via thermal decomposition of magnesium oxalate. J Phys Chem Solids 2010. doi: https://doi.org/10.1016/j.jpcs.2010.08.014.
[42] Salavati-Niasari M, Loghman-Estarki MR, Davar F. Controllable synthesis of nanocrystalline CdS with different morphologies by hydrothermal process in the presence of thioglycolic acid. Chem Eng J 2008. doi: https://doi.org/10.1016/j.cej.2008.08.040.
[43] Salavati-Niasari M. Synthesis and characterization of host (nanodimensional pores of zeolite-Y)–guest [unsaturated 16-membered octaaza–macrocycle manganese (II), cobalt (II), nickel (II), copper (II), and zinc (II) complexes] nanocomposite materials. Chem Lett 2005;34:1444–5.
[44] Sambhy V, MacBride MM, Peterson BR, Sen A. Silver bromide nanoparticle/polymer composites: Dual action tunable antimicrobial materials. J Am Chem Soc 2006. doi: https://doi.org/10.1021/ja061442z.
[45] Bar H, Bhui DK, Sahoo GP, Sarkar P, De SP, Misra A. Green synthesis of silver nanoparticles using latex of Jatropha curcas. Colloids Surf, A 2009. doi: https://doi.org/10.1016/j.colsurfa.2009.02.008.
[46] Li S, Shen Y, Xie A, Yu X, Qiu L, Zhang L, et al. Green synthesis of silver nanoparticles using Capsicum annuum L. Extract. Green Chem 2007. doi: https://doi.org/10.1039/b615357g.
[47] Ahmed S, Saifullah, Ahmad M, Swami BL, Ikram S. Green synthesis of silver nanoparticles using Azadirachta indica aqueous leaf extract. J Radiat Res Appl Sci 2016. doi: https://doi.org/10.1016/j.jrras.2015.06.006.
[48] Awwad AM, Salem NM, Abdeen AO. Green synthesis of silver nanoparticles using carob leaf extract and its antibacterial activity. Int J Ind Chem 2013. doi: https://doi.org/10.1186/2228-5547-4-29.
[49] Liao S, Wang W, Uo M, Ohkawa S, Akasaka T, Tamura K, et al. A three-layered nano-carbonated hydroxyapatite/collagen/PLGA composite membrane for guided tissue regeneration. Biomaterials 2005. doi: https://doi.org/10.1016/j.biomaterials.2005.05.050.
[50] Nublat C, Braud C, Garreau H, Vert M. Ammonium bicarbonate as porogen to make tetracycline-loaded porous bioresorbable membranes for dental guided tissue regeneration: Failure due to tetracycline instability. J Biomater Sci Polym Ed 2006. doi: https://doi.org/10.1163/156856206778937262.
[51] Zhang S, Huang Y, Yang X, Mei F, Ma Q, Chen G, et al. Gelatin nanofibrous membrane fabricated by electrospinning of aqueous gelatin solution for guided tissue regeneration. J Biomed Mater Res Part A 2009. doi: https://doi.org/10.1002/jbm.a.32136.
[52] Subbiah T, Bhat GS, Tock RW, Parameswaran S, Ramkumar SS. Electrospinning of nanofibers. J Appl Polym Sci 2005. doi: https://doi.org/10.1002/app.21481.
[53] Pham QP, Sharma U, Mikos AG. Electrospinning of polymeric nanofibers for tissue engineering applications: A review. Tissue Eng 2006. doi: https://doi.org/10.1089/ten.2006.12.1197.
[54] Pham QP, Sharma U, Mikos AG. Electrospun poly (ε-caprolactone) microfiber and multilayer nanofiber/microfiber scaffolds: Characterization of scaffolds and measurement of cellular infiltration. Biomacromolecules 2006. doi: https://doi.org/10.1021/bm060680j.

[55] Pang YX, Bao X. Influence of temperature, ripening time and calcination on the morphology and crystallinity of hydroxyapatite nanoparticles. J Eur Ceram Soc 2003. doi: https://doi.org/10.1016/S0955-2219(02)00413-2.
[56] Mobasherpour I, Heshajin MS, Kazemzadeh A, Zakeri M. Synthesis of nanocrystalline hydroxyapatite by using precipitation method. J Alloy Compd 2007. doi: https://doi.org/10.1016/j.jallcom.2006.05.018.
[57] Wang P, Li C, Gong H, Jiang X, Wang H, Li K. Effects of synthesis conditions on the morphology of hydroxyapatite nanoparticles produced by wet chemical process. Powder Technol 2010. doi: https://doi.org/10.1016/j.powtec.2010.05.023.
[58] Meng ZX, Zheng W, Li L, Zheng YF. Fabrication and characterization of three-dimensional nanofiber membrance of PCL-MWCNTs by electrospinning. Mater Sci Eng, C 2010. doi: https://doi.org/10.1016/j.msec.2010.05.003.
[59] Li Z, Yubao L, Aiping Y, Xuelin P, Xuejiang W, Xiang Z. Preparation and in vitro investigation of chitosan/nano-hydroxyapatite composite used as bone substitute materials. J Mater Sci – Mater Med 2005. doi: https://doi.org/10.1007/s10856-005-6682-3.
[60] Xu X, Yang Q, Wang Y, Yu H, Chen X, Jing X. Biodegradable electrospun poly(l-lactide) fibers containing antibacterial silver nanoparticles. Eur Polym J 2006. doi: https://doi.org/10.1016/j.eurpolymj.2006.03.032.
[61] Hong KH, Park JL, Hwan Sul IN, Youk JH, Kang TJ. Preparation of antimicrobial poly(vinyl alcohol) nanofibers containing silver nanoparticles. J Polym Sci, Part B: Polym Phys 2006. doi: https://doi.org/10.1002/polb.20913.
[62] Rao VB, Prasad KG, Naragani K, Muvva V. Screening and antimicrobial activity of actinomycetes isolated from the rhizosphere of Clitoria ternatea. J Nature Natural Sci 2016. doi: https://doi.org/10.26859/jnnsci.v1i01.9591.
[63] Debnath T, Ghosh S, Potlapuvu US, Kona L, Kamaraju SR, Sarkar S, et al. Proliferation and differentiation potential of human adipose-derived stem cells grown on chitosan hydrogel. PLoS ONE 2015. doi: https://doi.org/10.1371/journal.pone.0120803.
[64] Sculean A, Nikolidakis D, Schwarz F. Regeneration of periodontal tissues: Combinations of barrier membranes and grafting materials – Biological foundation and preclinical evidence: A systematic review. J Clin Periodontol 2008. doi: https://doi.org/10.1111/j.1600-051X.2008.01263.x.
[65] Nyman S, Lindhe J, Karring T, Rylander H. New attachment following surgical treatment of human periodontal disease. J Clin Periodontol 1982. doi: https://doi.org/10.1111/j.1600-051X.1982.tb02095.x.
[66] Geurs NC, Korostoff JM, Vassilopoulos PJ, Kang T-H, Jeffcoat M, Kellar R, et al. Clinical and histologic assessment of lateral alveolar ridge augmentation using a synthetic long-term bioabsorbable membrane and an allograft. J Periodontol 2008. doi: https://doi.org/10.1902/jop.2008.070595.
[67] Behring J, Junker R, Walboomers XF, Chessnut B, Jansen JA. Toward guided tissue and bone regeneration: Morphology, attachment, proliferation, and migration of cells cultured on collagen barrier membranes. A systematic review. Odontology. 2008. doi: https://doi.org/10.1007/s10266-008-0087-y.
[68] Taba J, Jin Q, Sugai JV, Giannobile WV. Current concepts in periodontal bioengineering. Orthod Craniofac Res 2005. doi: https://doi.org/10.1111/j.1601-6343.2005.00352.x.
[69] Bottino MC, Jose MV, Thomas V, Dean DR, Janowski GM. Freeze-dried acellular dermal matrix graft: Effects of rehydration on physical, chemical, and mechanical properties. Dent Mater 2009. doi: https://doi.org/10.1016/j.dental.2009.03.007.
[70] Bottino MC, Thomas V, Schmidt G, Vohra YK, Chu TMG, Kowolik MJ, et al. Recent advances in the development of GTR/GBR membranes for periodontal regeneration – A materials perspective. Dent Mater 2012. doi: https://doi.org/10.1016/j.dental.2012.04.022.
[71] Rujitanaroj P, Pimpha N, Supaphol P. Wound-dressing materials with antibacterial activity from electrospun gelatin fiber mats containing silver nanoparticles. Polymer 2008. doi: https://doi.org/10.1016/j.polymer.2008.08.021.
[72] Junqueira LCU, Carneiro J. Basic histology: text & atlas. McGraw-Hill Professional; 2005.
[73] Johansen E, Parks HF. Electron microscopic observations on the three-dimensional morphology of apatite crystallites of human dentine and bone. J Biophys Biochem Cytol 1960. doi: https://doi.org/10.1083/jcb.7.4.743.
[74] Rahisuddin Akrema. Extracellular synthesis of silver dimer nanoparticles using Callistemon viminalis (bottlebrush) extract and evaluation of their antibacterial activity. Spectrosc Lett 2016. doi: https://doi.org/10.1080/00387010.2016.1140654.
[75] Shameli K, Bin Ahmad M, Yunus WMZW, Rustaiyan A, Ibrahim NA, Zargar M, et al. Green synthesis of silver/montmorillonite/chitosan bionanocomposites using the UV irradiation method and evaluation of antibacterial activity. Int J Nanomed 2010. doi: https://doi.org/10.2147/IJN.S13632.
[76] Murugan R, Ramakrishna S. Nano-featured scaffolds for tissue engineering: A review of spinning methodologies. Tissue Eng 2006. doi: https://doi.org/10.1089/ten.2006.12.435.
[77] Kokubo T, Takadama H. How useful is SBF in predicting in vivo bone bioactivity?. Biomaterials 2006. doi: https://doi.org/10.1016/j.biomaterials.2006.01.017.
[78] Kokubo T. Apatite formation on surfaces of ceramics, metals and polymers in body environment. Acta Mater 1998. doi: https://doi.org/10.1016/S1359-6454(98)80036-0.
[79] Chung RJ, Hsieh MF, Huang CW, Perng LH, Wen HW, Chin TS. Antimicrobial effects and human gingival biocompatibility of hydroxyapatite sol-gel coatings. J Biomed Mater Res – Part B Appl Biomater 2006. doi: https://doi.org/10.1002/jbm.b.30365.
[80] Frenot A, Chronakis IS. Polymer nanofibers assembled by electrospinning. Curr Opin Colloid Interface Sci 2003. doi: https://doi.org/10.1016/S1359-0294(03)00004-9.
[81] Shah D, Maiti P, Jiang DD, Batt CA, Giannelis EP. Effect of nanoparticle mobility on toughness of polymer nanocomposites. Adv Mater 2005. doi: https://doi.org/10.1002/adma.200400984.
[82] Song X, Ling F, Ma L, Yang C, Chen X. Electrospun hydroxyapatite grafted poly (l-lactide)/poly(lactic-co-glycolic acid) nanofibers for guided bone regeneration membrane. Compos Sci Technol 2013. doi: https://doi.org/10.1016/j.compscitech.2013.02.014.
[83] Guzman M, Dille J, Godet S. Synthesis and antibacterial activity of silver nanoparticles against gram-positive and gram-negative bacteria. Nanomed Nanotechnol Biol Med 2012. doi: https://doi.org/10.1016/j.nano.2011.05.007.
[84] Speranza G, Gottardi G, Pederzolli C, Lunelli L, Canteri R, Pasquardini L, et al. Role of chemical interactions in bacterial adhesion to polymer surfaces. Biomaterials 2004. doi: https://doi.org/10.1016/j.biomaterials.2003.08.061.
[85] Feng QL, Wu J, Chen GQ, Cui FZ, Kim TN, Kim JO. A mechanistic study of the antibacterial effect of silver ions on Escherichia coli and Staphylococcus aureus. J Biomed Mater Res 2000. doi: https://doi.org/10.1002/1097-4636(20001215)52:4<662::AID-JBM10>3.0.CO;2-3.
[86] Murray RG, Steed P, Elson HE. The location of the mucopeptide in sections of the cell wall of *Escherichia coli* and other gram-negative bacteria. Can J Microbiol 1965. doi: https://doi.org/10.1139/m65-072.
[87] Raffi M, Hussain F, Bhatti TM, Akhter JI, Hameed A, Hasan MM. Antibacterial characterization of silver nanoparticles against E. coli ATCC-15224. J Mater Sci Technol 2008.
[88] Shockman GD, Barren JF. Structure, function, and assembly of cell walls of gram-positive bacteria. Annu Rev Microbiol 1983. doi: https://doi.org/10.1146/annurev.mi.37.100183.002441.
[89] Kumar A, Vemula PK, Ajayan PM, John G. Silver-nanoparticle-embedded antimicrobial paints based on vegetable oil. Nat Mater 2008. doi: https://doi.org/10.1038/nmat2099.
[90] Kim J-S. Antibacterial activity of Ag+ ion-containing silver nanoparticles prepared using the alcohol reduction method. J Ind Eng Chem 2007;13:718–22.
[91] Gordon MY, Levičar N, Pai M, Bachellier P, Dimarakis I, Al-Allaf F, et al. Characterization and clinical application of human CD34 + stem/progenitor cell populations mobilized into the blood by granulocyte colony-stimulating factor. Stem Cells 2006. doi: https://doi.org/10.1634/stemcells.2005-0629.
[92] Bhumiratana S, Vunjak-Novakovic G. Concise review: personalized human bone grafts for reconstructing head and face. Stem Cells Translat Med 2012. doi: https://doi.org/10.5966/sctm.2011-0020.
[93] Caplan AI. Adult mesenchymal stem cells for tissue engineering versus regenerative medicine. J Cell Physiol 2007. doi: https://doi.org/10.1002/jcp.21200.
[94] Busa WB, Nuccitelli R. Metabolic regulation via intracellular pH. Am J Physiol – Regulat Integr Comparat Physiol 1984. doi: https://doi.org/10.1152/ajpregu.1984.246.4.r409.
[95] Ferraz MP, Monteiro FJ, Manuel CM. Hydroxyapatite nanoparticles: a review of preparation methodologies. J Appl Biomater Biomech 2004;2:74–80.